# Development of a Prototype Underwater Test Platform for the Low Reynolds Number Regime

Cody J. Karcher[1] and Derek A. Paley, Ph.D.[2]
*University of Maryland, College Park, MD, 20742*

**This paper will detail the design, construction and testing of a prototype underwater vehicle. This vehicle was designed to match the Reynolds number of a Micro Air Vehicle (MAV), so that future experiments can be performed to analyze the aerodynamic and control properties of the vehicle and by extension, an MAV. Preliminary design will be discussed, along with a brief synopsis of design decisions based on mission criteria. Construction methods will be described, including the assembly of a pressure vessel necessary for operating in the underwater environment and work with carbon composite materials to build the aerodynamic surfaces of the vehicle. Testing methodology to determine moments of inertia will be shown and data analysis will be presented. Flight testing will be documented, along with a qualitative description of the vehicle's performance and handling qualities. Future work will be described and conclusions presented.**

## Nomenclature

| | | |
|---|---|---|
| $c$ | = | Chord Length |
| $d$ | = | Distance Between Bifilar Pendulum Strings |
| $F_B$ | = | Buoyant Force Acting on an Object |
| $g$ | = | Gravitational Constant of Earth |
| $h$ | = | Height of the Bifilar Pendulum |
| $I$ | = | Local Moment of Inertia |
| $I_{xx}$ | = | Moment of Inertia About Roll Axis |
| $I_{yy}$ | = | Moment of Inertia About Pitch Axis |
| $I_{zz}$ | = | Moment of Inertia About Yaw Axis |
| $I_{xy}$ | = | Moment of Inertia for Roll-Pitch Coupling |
| $I_{xz}$ | = | Moment of Inertia for Roll-Yaw Coupling |
| $I_{yz}$ | = | Moment of Inertia for Pitch-Yaw Coupling |
| $m$ | = | Mass |
| $\mu$ | = | Dynamic Viscosity |
| $Re$ | = | Reynolds Number |
| $\rho$ | = | Density |
| $u$ | = | Velocity |
| $V$ | = | Volume |
| $\omega$ | = | Frequency |

## I. Motivation

IN recent years, there has been a strong push in the aeronautics community to develop small-scale flying machines. These so called Micro Air Vehicles (MAVs) have several applications in both civilian and military arenas. In the civilian arena, some companies have recently published a concept for a package delivery system using MAVs. However, the most prolific use of MAVs will likely be in the military sector. Low power requirements and small size make these vehicles inexpensive to build and operate, and low noise emissions and surveillance abilities make

[1] Undergraduate Research Assistant, Department of Aerospace Engineering, 3181 Glenn L. Martin Hall, AIAA Student Member, ckarcher@terpmail.umd.edu
[2] Associate Professor, Department of Aerospace Engineering, 3181 Glenn L. Martin Hall, AIAA Associate Fellow

them highly useful battlefield equipment.[1] These traits have led the University of Maryland to pursue a number of research projects with the purpose of investigating the construction and testing of these vehicles.

In addition, the underwater environment has become an increasingly active area of interest for aerospace research. One of the most well known underwater research facilities is NASA's Neutral Buoyancy Facility at the Johnson Space Flight Center, a facility which has become crucial in the testing of space vehicles. However, the underwater environment has become increasingly used in other research areas, such as flow sensing, flow visualization, and control algorithm tests.

**Figure 1. Neutral Buoyancy Research Facility (NBRF) at the University of Maryland** *(Author's Personal Collection)*

The Collective Dynamics and Control Laboratory (CDCL) at the University of Maryland is uniquely positioned to bridge these two active research areas. The lab has been doing research with underwater vehicles since the founding of the lab, thanks to an underwater motion capture facility located in an on campus neutral buoyancy facility (Fig. 1). In large part, the goal of this project was to simply build a vehicle capable of taking advantage of this facility. Research in the lab also typically focuses on how to expand the functionality of existing MAVs for the purposes of multi-vehicle operations. This work seemed a natural extension of both of these areas of research.

## II. History

The CDCL has worked for a number of years with the Sea Perch underwater platform (Fig. 2). These vehicles have a relatively simple control scheme, being neutrally buoyant and with three perpendicular motors to control X, Y and Z axes. While traditionally these vehicles are tethered to power at the surface, researchers at the CDCL have developed a version which is untethered and is controlled by a computer via an RC connection. The advantage of these vehicles is that they provide a very robust and well-tested platform for testing control algorithms. The authors set out with the goal of developing a new vehicle that would closer simulate the dynamics of an air vehicle and also be developed into a platform as robust as the Sea Perch.

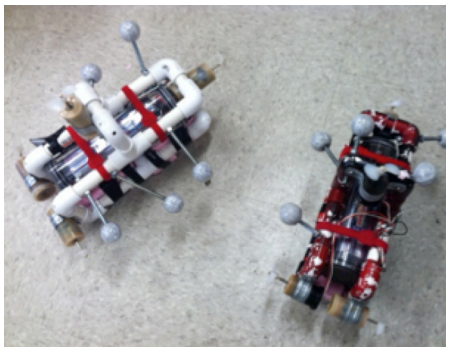

**Figure 2. Sea Perch Vehicles** *(Courtesy of the UMD CDCL)*

While the Sea Perch provided a target mission, the Poseidon vehicle (Fig. 3) provided the opportunity to develop many of the construction methods which would be used for the Low Reynolds Number Project. The mission for Poseidon was to create a vehicle which required only a single control input (speed) to control its navigation to any waypoint in a given X-Y plane (plane with constant altitude).

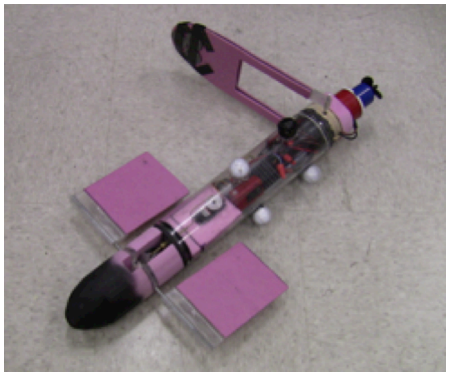

**Figure 3. The Poseidon Vehicle** *(Author's Personal Collection)*

The vehicle design was to be as simple as possible. A cylindrical pressure vessel was needed to protect the electronics of the vehicle, and so this pressure vessel doubled as the fuselage. A fin was developed which provided a turning rate which was dependent on the speed of the vehicle.

Ultimately, the vehicle was constructed such that two control inputs, speed and elevator, could be used to accomplish the desired mission. The Poseidon vehicle was successfully flight-tested on a number of occasions, however, it was soon shelved to pursue other endeavors.

## III. Design

The mission contrived by the authors primarily drove design decisions for this vehicle. Some of these criteria have been previously mentioned, but are listed here for completeness:

1) The vehicle should have the same Reynolds number as a reasonably sized MAV. Reynolds number of approximately 50,000 was selected as a good target value. This is comparable to an MAV with a chord of 9 inches traveling at 7.5 ft/s in air.
2) The vehicle should generate a lifting force as a result of fluid motion rather than relying on neutral buoyancy or an unbalanced buoyant force.
3) The vehicle should have as few control inputs as possible. This limits the complexity of the pressure vessel as well as the control algorithm.
4) The wingspan was constrained to be two feet in order to fit into other UMD testing facilities.
5) The vehicle should be mechanically operational up to depths of at least 20 feet of water (approximately 1.6 atm of pressure)

### A. Quirks of the Underwater Environment

Perhaps the most obvious challenge with underwater robotics is that electricity and water do not tend to mix well. In order to combat this challenge, all electrical components are placed into a pressure vessel, protecting them from harm beyond a depth of 30 feet, which is the maximum depth of the testing facility.

While electricity and power are the most obvious challenge, perhaps the biggest challenges of working in the underwater environment is battling buoyancy. Many hours in the lab were spent attempting to fine-tune this particularly nasty parameter. In many applications, buoyant force is a friend to the researcher, and as will be seen in later discussion, proved useful for this research as well. Buoyant force acts in direct opposition to gravity and is subject to Archimedes's Principle[2]:

$$F_B = \rho g V \tag{1}$$

The easiest way to visualize this equation is to realize that the buoyant force is equivalent to the weight of water being displaced by an object. Thus, while the weight of an object is a function of mass by Newton's Second Law, the buoyancy of an object is a function of volume by Archimedes's Principle.

Additionally, the increased pressure of the underwater environment leads to a number of problems as well. These problems become most evident when using foam for construction. Foam is generally used to make a negatively buoyant vehicle more positively buoyant when working underwater, however, most foams, including the expanded and extruded polystyrene foams used for this research, compress in high pressure environments. When the foam compresses, this decreases the volume of the vehicle and thereby the buoyant force, so it is easy to imagine a scenario, indeed it has happened on many occasions in this research, where a vehicle gets too deep, resulting in foam compression to the point that the decreased volume no longer provides sufficient buoyant force to return the vehicle to the surface. Unfortunately, since most of these vehicles operate very close to neutral buoyancy, this frequently results in many hours of attempting to retrieve vehicles from the bottom of the 30-foot research tank in Fig. 1.

### B. Preliminary Design

Design began with a conventional aircraft configuration, with fuselage, wings horizontal stabilizer and vertical stabilizer (Fig. 4). However, desire to simplify the design quickly eliminated the horizontal stabilizer with an elevator in favor of a configuration using elevons for both pitch and roll control. While early designs included a rudder for directional control, it was determined that differential elevon control would suffice to eliminate adverse yaw during turning, and so in an effort to further simplify the design, the rudder was eliminated as well. As was mentioned previously, a circular pressure vessel doubled as fuselage.

**Figure 4. Example of a Conventional Aircraft Configuration** *NASA's DROID Flight Research Platform (Author's Personal Collection)*

Actuating these elevons proved somewhat challenging within the constraints of the pressure vessel. Traditionally, in hobby RC aircraft, a servo is placed directly forward of a control surface, and would in the case of the vehicle in Figure 4, be embedded in the wing. By actuating the servo linearly, a push rod moves a control horn directly connected to the control surface. However, this

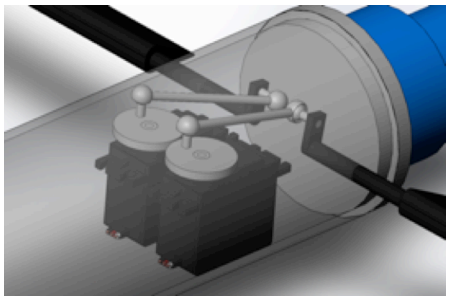

**Figure 5. Layout of the Servos and Control Horns for the Elevons**

was unfeasible due to the fact that servos had to be contained within the pressure vessel, and in this placement, it would be impractical to attempt direct linear actuation in this fashion while still maintaining the integrity of the pressure vessel. Thus, it became necessary to develop a new actuation scheme. By moving the control horns into the pressure vessel and only running out a single rotating steel shaft for each elevon, it was easy to maintain pressure vessel integrity and still provide adequate control actuation (Fig. 5).

With a limitation on span of 24 inches, a chord length of 6 inches was selected to maintain a reasonable aspect ratio on the wing. This selection put the velocity of the vehicle at approximately 1 ft/s in order to attain a Reynolds number of 50,000. This parameter is determined from the following equation[2]:

$$\mathrm{Re} = \frac{\rho u c}{\mu} \tag{2}$$

From previous experience with Poseidon, it was known that 1 ft/s was an attainable goal, and so the design proceeded with this geometry. However, the span was dropped even further to 20 inches in a further effort to accommodate a new facility under construction, which would only be able to fit this size of vehicle. Next, taper was added for aesthetic value, resulting in a linear taper from 7 inches down to 5 inches.

Airfoil selection was driven by two primary factors. First, a thick airfoil was desired, as much of the actuation for the vehicle would have to take place within the wing itself. A secondary requirement was to look for reasonable performance at low Reynolds numbers. With these two criteria in mind, the NACA 4421 airfoil was selected.

Few structural components had to be considered with this vehicle, with the most notable element being the wing. Due to previous carbon composite experience, a carbon-foam sandwich structure was proposed for the wing. This construction led to some difficulty, as the large foam block of the wing provided a large buoyant force, but this foam could be hollowed out and replaced with lead shot in order to provide sufficient negative buoyancy. The difficulty came then with integrating the rotating shafts for the elevons with the wing itself. The shaft was designed to actually pass through the trailing edge of the wing in a manner that will be further described in the Construction section. The elevons themselves were also designed to be covered with carbon fiber.

To propel the vehicle, the exact same setup that was used for Poseidon was designed, as it had proven reliable on this vehicle. A Rule Bilge Pump was modified to create a waterproof motor in a process detailed at the website Homebuilt ROV's. A Graupner G230850 3 bladed 50mm propeller was used.

With these various pieces of information, a CAD model was constructed in SolidWorks in order to detail the design of various controls and provide a platform for the simulation section detailed in a later section (Fig. 6). The CAD model also provided a platform for testing various pressure vessel layouts. At this stage, it became apparent that an off-the-shelf battery pack would not meet the dimensional requirements for this vehicle, and so one was designed using individually available batteries. Also, placement of various internal components such as the speed controller and servos was determined, however, much of this changed during the construction phase in an effort to fit all of the components into the vessel.

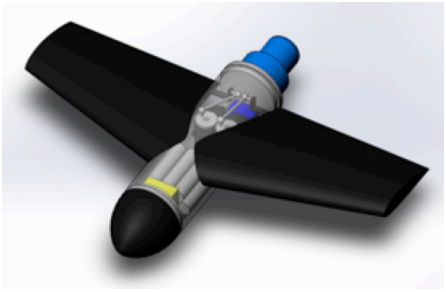

**Figure 6. CAD Model of the Vehicle**

At this point in the design, two major features would change during construction: in the model, there is a 6° angle of incidence, and the wings are mounted to provide lift in the upward direction. Details of these two design variables will be detailed in the Construction section below.

## IV. Simulation

Before constructing the vehicle, it was necessary to perform a number of simulation runs in order to give an estimate of vehicle performance. The SolidWorks Flow Simulation package was used to generate pressure plots and document lift, drag and control moments. For the purposes of design validation, three runs were considered important: steady level flight, roll, and pitch. All runs were done with the following conditions:

Working Fluid: Water
Flow Velocity: 12 in/s in the direction nose to tail
Ambient Pressure: 21 lbf/in$^2$ (Approximately 15 ft. depth)
Temperature: 90 °F

As this is not a simulation paper, nor is this a simulation study, these simulation runs are rather imprecise and would leave much to be desired for one whose specialty is modeling or computation, however, it proved more than enough to validate the design and proceed with construction.

### A. Steady Level Flight

This run had no surface deflection and was done for the sole purpose of demonstrating that the vehicle was capable of generating lift at zero angle of attack. Results are as follows:

Lift: 0.1962 lbf
Drag: 0.04915 lbf
Pitching Moment: 0.9345 in-lbf (nose down)

These results showed the expected results. Pressure was lower along the top of the wing, resulting in a lifting force. While the total lift ended up being less than a pound of force, increasing angle of attack easily generates more lift.

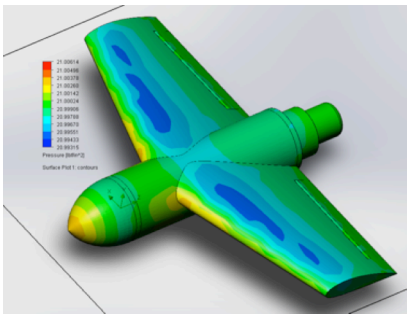

**Figure 7. Local Relative Pressure for a Steady Level Flight Condition**

### B. Pitch

For this run, the two elevons were deflected to generate the maximum nose-down pitching moment that the design would allow. The goal was to determine if deflecting the surfaces could in fact generate a pitching moment. Results are as follows:

Lift: 0.3394 lbf
Drag: 0.7638 lbf
Pitching Moment: 1.7333 in-lbf (nose down)

These results are again consistent with expectations. An increase in total lift is observed, and the pitching moment increased in the correct direction.

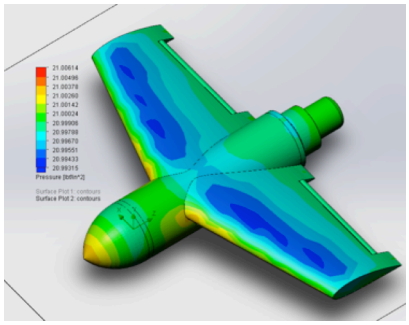

**Figure 8. Local Relative Pressure for a Pitch Down Maneuver**

### C. Roll

For this run, the two elevons were deflected to generate the maximum left wing down rolling moment that the design would allow. The goal was to determine if deflecting the surfaces could in fact generate a rolling moment. Results are as follows:

Rolling Moment: 0.3547 in-lbf

Once again, the results show a roll in the correct direction. Note the increase in pressure on the vehicle's left wing and expansion of the blue low pressure region on the right wing.

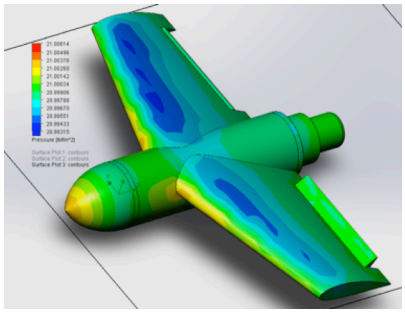

**Figure 9. Local Relative Pressure for a Left Roll Maneuver**

## V. Construction

### A. Pressure Vessel

The pressure vessel is a hard plastic molded cylinder available from Mike's Subworks online store. Based on the CAD model, a measurement was made to determine where holes should be drilled for the elevon actuation rods, then, these holes were drilled straight through the pressure vessel on a manual mill. Brass seals were then glued into the holes with cyanoacrylic, parts also available at Mike's Subworks. Eighth inch stainless steel shaft was then cut to length and inserted through these seals. A foam insert was manufactured to house the servomotors, and then the servomotors were then glued into place with hot glue. Brass control rods were then bent into a shape which would allow for the servos to actuate and provide adequate deflection of the control surfaces and attached to the servomotors. This assembly was then hot glued into the pressure vessel. Control horns were then manufactured to attach to the steel elevon shafts. At this point, it really became a "ship in a bottle" process of simply attempting to get all the components together so that the servos would actuate the elevons as intended. The battery was then assembled using ten 1.2 volt rechargeable NiMH batteries, small strands of wire, solder and electrical tape, and inserted up against the foam insert for the servos. NiMH batteries had to be used as a policy in the NBRF forbids lithium batteries. Finally, the smaller components, including the speed controller and RC receiver were placed in the remaining space.

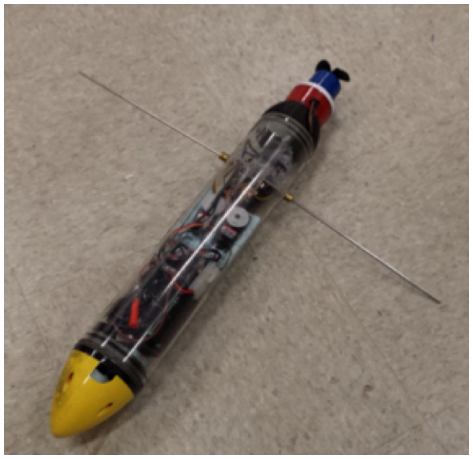

**Figure 10. Pressure Vessel without Wings**

### B. Thruster

The housing of the bilge pump was removed using a hacksaw, and the propeller simply glued onto the rotating stem with cyanoacrylic. As mentioned above, this process is detailed at the website Homebuilt ROVs. A fuse was also soldered into the high voltage line in an effort to protect the electronics in the event of a leak. The wires for the thruster were run up past the control horns and servomotors to the front of the pressure vessel so that they could connect to the speed controller, as the short wires on the speed controller required it to be in close proximity to the battery, which had been placed at the front of the pressure vessel during the CAD modeling stage. In the first major deviation from the CAD model, a 3D printed piece of approximately 2 inches in length was inserted between the thruster and the end cap of the pressure vessel. This gave enough clearance to the wires of the thruster, which had to enter the pressure vessel through the end cap, and so, in order for the thruster to sit flush on the endcap, some additional space was required. The end cap-spacer-thruster assembly was glued together with hot glue and from that point on considered to be one piece.

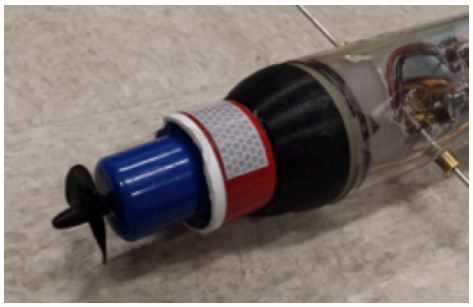

**Figure 11. Thruster and Spacer Assembly** *Note the black spacer between the red motor and beige endcap. The white golf ball pattern is a marker used for motion capture.*

### C. Wings

Extruded polystyrene foam was cut on a foam cutter into the shape of each wing using the NACA 4421 profile and appropriate taper ratio. These wing forms became the foam cores for the wings and elevons. A box cutter was then used to remove the elevons, with the size of the control surface being dictated by the CAD model. The hinge line for the elevons was then laid out based on the new "hole" in the trailing edge. A crafting hot wire tool was used to create oversized holes in the approximate location of the control rod in both the inboard and outboard sections of the wing. Small delrin tube pieces were then epoxied into place in these holes, using spare steel shaft to ensure alignment (Fig. 12). The inner diameter of these tubes had been drilled out to be slightly oversized so that the control shaft could rotate freely.

The foam cores were then wrapped in carbon fabric and attached to the pressure vessel in a single composite layup. This provided a convenient means to attach the wing without compromising the integrity of the pressure vessel. The pressure vessel was first wrapped in release so that the wings could later removed from the vehicle to ease future work in the pressure vessel. This release was then wrapped in 0-90 weave carbon fabric and taped into place. Next, the foam wings were inserted onto the control rods which were sticking out of the fuselage in order to provide proper alignment. These wings were then covered in the same fabric, which was again taped into place. At this point, 30-minute epoxy was applied to the carbon fiber, but not allowed to set before strips of fabric were applied to join the carbon on the pressure and the carbon on the wing. These strips were covered in epoxy before they were applied. The fabric was smoothed as much as possible and then placed in a vacuum bag to cure. At this point, it was decided to simply leave the wings at zero degrees angle of incidence, as adding the originally planned 6 degrees would prove to be difficult with the given setup. The result of this layup was rather messy and provided a poor aerodynamic surface, however, it provided the necessary structural framework, and the aerodynamics were corrected later in the process.

**Figure 12. Delrin Spacer** *This spacer (white object, center) is the outboard pivot point for the left aileron.*

**Figure 13. Vacuum Bag** *The vehicle in the process of being vacuum bagged while the composite wraps set*

After the vehicle was removed from the vacuum bag, a seam was dremeled down the length of the circular piece so that the wings could be removed from the vehicle. Once the wings had been removed, the hot wire was once again used to hollow out a large portion of each wing. This was done in a rough effort to duplicate the location of a wing box spar in a normal wing. These sections were then filled with lead shot, and set in with epoxy, forming a heavy solid block within each wing. These two blocks provided most of the vehicle's negative buoyancy. After vacuum bagging the vehicle, the trailing edges of the airfoils were rounded and not aerodynamic. Thus, these sections of the carbon fiber were cut away from the foam core and replaced with new carbon fiber strips and set in place with 5-minute epoxy. At this point, the surfaces of the wings still had numerous wrinkles and other flow trips which would cause turbulent flow. To correct these problems, Bondo was applied to the wings and sanded down, providing smooth laminar surfaces.

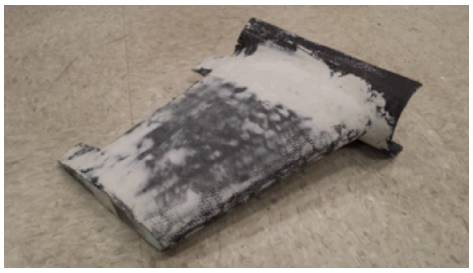

**Figure 14. Wing** *The wing in its final constructed state. Black is the composite showing through the added white Bondo*

**D. Elevons**

The pieces which had been cut away from the wings were used as the blanks for these control surfaces. The leading corners were cut away to allow for clearance during actuation. Using the hot wire, a channel was cut in leading surface of the wedge shape. This allowed for the attachment of delrin tube which would fit around the control shaft. This delrin was selected so the inner diameter would fit onto the shaft, however, the fit was left snug so that the surface could not rotate independently of the shaft. However, small shaft collars were also attached to the delrin tube to fix the surfaces onto the shafts. This setup was used so that the surfaces would be removable for maintenance, rather than just gluing them directly onto the shafts themselves. Finally, Bondo was used to cover the elevons in a hard coating to make them more durable, replacing the originally planned carbon fiber.

**Figure 15. Elevon**

### E. Assembly

With all parts complete, assembly was straightforward. A change was made from the original design, in that the wings were mounted upside down. By making this change, the vehicle could be positively buoyant and the lifting force would "pull" the vehicle underwater, a highly preferable situation to a negatively buoyant vehicle. Duct tape was used to hold the wings onto the pressure vessel because it was easy to put on and take off. For some of the later tests, a salvage hook was also attached to the top of the vehicle to ease rescue operations. Final mass data for the vehicle is recorded in Table 1 of Appendix I and is used below in the Testing section.

**Figure 16. Final Vehicle Assembly**

### F. Buoyancy

Small packets were made of leftover lead shot and duct tape and placed into the pressure vessel, and by varying the weight in these packets, proper buoyancy was achieved by trial and error. The vehicle was rather close to neutral buoyancy, which takes away some of the ability to simulate real flow conditions, however, at this point in the project, it was more desirable to have a highly maneuverable and retrievable vehicle. Changes to this scenario will be discussed in the Future Work section.

## VI. Testing

### A. Moment of Inertia (MOI) Testing

Moment of inertia values are desirable due to their importance in determining stability and control matrices from flight data. Initial CAD drawings were not done with enough detail to provide sufficiently accurate values, and so the moments of inertia were determined experimentally. For this size of vehicle, a common method for determining principal moments of inertia is the bifilar pendulum (Fig. 17). In this setup, the vehicle is hung from two strings, and a step response excites the natural frequency of the rotating body. By measuring a few parameters, one can determine the moment of inertia by using the following equaiton[3]:

$$I = \frac{mgd^2}{16\pi h\omega^2} \qquad (3)$$

**Figure 17. Vehicle on the Bifilar Pendulum** *Vehicle at approximately -45° pitch during the $I_{xx}$, $I_{zz}$ and $I_{xz}$ test.*

Thus, by suspending the vehicle such that it rotates about the three geometrically defined aircraft axes, it is easy to experimentally determine $I_{xx}$, $I_{yy}$, and $I_{zz}$. Due to symmetry, it is apparent for this vehicle that $I_{xy}$ and $I_{yz}$ are zero. However, $I_{xz}$ will be non-zero. To determine $I_{xz}$, the vehicle was rotated through multiple pitch attitudes and swung on the bifilar pendulum. This process should in theory produce a portion of a sinusoidal wave that is predicted by Mohr's Circle for moment of inertias (Fig. 18). However, it will be out of phase by a certain phase angle, corresponding to the angle between the principal axes and the geometrically defined axes. Note in Fig. 18 that the green lines indicate principal axes, the red the geometric axes, the phase difference of 2ϕ and that $I_{xx}$ and $I_{zz}$ are along the horizontal axis, while $I_{xz}$ is along the vertical axis. Data points were obtained for many pitch attitudes as described above in order to determine the moment of inertia at different angles. The data was then fitted to a cosine curve. Finally, the phase angle between a theoretical vehicle with $I_{xz}$ equal to zero and the fitted curve was determined. From this phase angle, $I_{xz}$ can be obtained using Mohr's Circle.

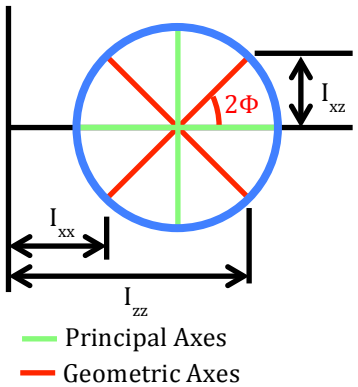


**Figure 18. Mohr's Circle for Moments of Inertia**

To determine the moments of inertia for the vehicle, first, the bifilar pendulum was set up to measure $I_{yy}$, or the moment of inertia about the pitching axis. Relevant measurements are documented in Table 2 in Appendix I. The

pendulum was excited and 10 cycles were measured and the time recorded. From this data, use of Eq. 3 results in an $I_{yy}$ of 0.8213 lbm-ft$^2$.

Next, the test was set up such that $I_{xx}$, $I_{zz}$, and $I_{xz}$ could be determined. Relevant measurements are documented in Table 3 in Appendix I. Then, the vehicle was fixed at pitch angles between -90° and 90° and the time for 8 cycles of the pendulum was measured. These results are shown in Table 3 in Appendix I. A MATLAB code was then written to determine the moments of inertia using the process described above. The first step is to determine the moment of inertia at each pitch angle and plot these results. Next, a cosine curve is fit to this data using a combination of error analysis and visual approximation. This fit varies the amplitude, phase and vertical shift of the cosine wave. This fitted curve is then plotted. Finally, this fitted curve is taken and the phase is fixed at zero degrees. This provides the theoretical MOI curve. These three plots are shown in Figure 19. From Mohr's Circle, it is apparent that $I_{zz}$ will be where the fitted cosine wave passes through an angle of 0° and that $I_{xx}$ will be where it crosses through the angle of 180°. Finally, $I_{xz}$ is the vertical component formed by Mohr's Circle for the calculated phase angle. Final results are as follows:

$I_{xx}$: 1.3814 lbm-ft$^2$
$I_{zz}$: 1.9598 lbm-ft$^2$
$I_{xz}$: 0.2251 lbm-ft$^2$

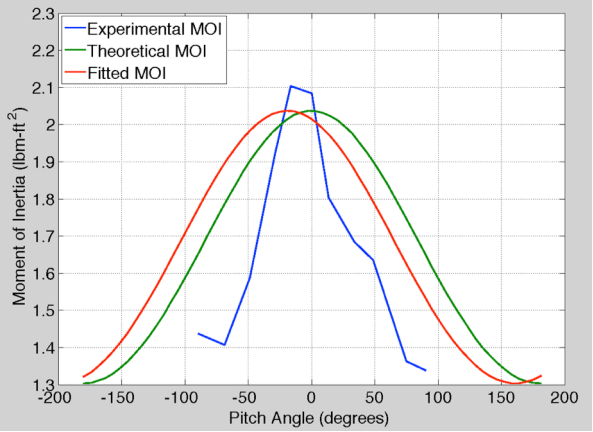


**Figure 19. Moment of Inertia vs. Pitch Angle for the Bifilar Pendulum** *The blue line shows experimental data, the green the theoretical wave produced by Mohr's circle and the red the fitted data.*

## B. Flight Testing

The purpose of flight-testing the vehicle was to assess its flight characteristics and determine its potential for use as a testbed in future CDCL projects. Perhaps the most common way to perform this task is by means of determining stability and control derivatives at different flight conditions and then assembling a database of stability and control matrices which can then be used to control the vehicle over the entire flight envelope. This type of analysis requires the accumulation of many different data points, including velocity, acceleration, orientation and control input data. The CDCL has a unique underwater motion capture facility which allows for the collection of this type of data[4], and the original goal was to use this system to assemble stability and control matrices. However, a major problem with working underwater is wireless communication. The motion capture area begins approximately 5 feet under the surface of the research tank and extends to approximately 20 feet of depth. However, as was determined by numerous flight-testing attempts, the communication between RC transmitter and receiver on the 72 MHz band was limited to a depth of 5 feet at optimal conditions, and no more than 2-3 feet during standard operations. While this range is based on observation in the lab, difficulties with underwater RC communication are well documented[5]. Thus, despite numerous attempts to get flight data, no test was successful in linking the data acquisition system to the vehicle. However, many successful flights were made piloting the vehicle with the RC transmitter directly to keep the vehicle in the 2-3 foot operational zone.

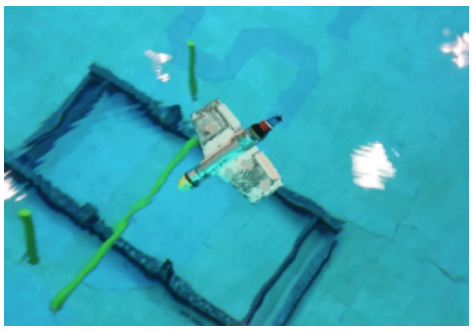

**Figure 20. Vehicle in Flight During Testing**

Initial testing showed the vehicle was particularly sensitive to the location of the center of gravity (CG). Too far forward, and the vehicle would nose down and the pilot would be unable to restore normal flight. However, too far back and the vehicle was uncontrollable. Perhaps the largest contribution to CG was the lead shot in the wings, however, the battery also provided a large component of the CG location. To fine-tune the location, the small bags of lead shot used to fine-tune the buoyancy were moved around within the pressure vessel, while foam spacers kept these bags and the other internal components secured in place. Trial and error was used to move the CG until the vehicle was flyable. While this likely changed the moments of inertia, due to changes of CG being very small, it was assumed that moments of inertia remaining mostly the same, with the major mass components remaining fixed. This

location turned out to be approximately 10.5 inches aft of the nose of the vehicle. For comparison, the aerodynamic center (AC) was located at approximately 11 inches back and roughly corresponds to the center of buoyancy as well, due to the fact that this point is also roughly at the center of the vehicle's planform geometry.

Once the CG was fixed into its proper location, the vehicle performed quite well in most handling qualities. Pitch response was somewhat slow, however, this was a desired trait in order to keep the vehicle at a relatively steady altitude to avoid loss of communication. Roll response was quite good, and by performing a bank followed by a pitch, the vehicle could accomplish turns with a very small turning radius. One interesting aspect of the vehicle is that the lack of vertical surfaces made it exceptionally unstable about the yaw axis (Fig. 21). However, this proved to be a rather fun challenge, and a little skill with the sticks could mitigate any difficulties. Future work may attempt to eliminate this phenomenon with the simple addition of a vertical surface, however, it is more likely that attempts will be made to resolve the issue as an interesting control problem. This should be possible, as adverse yaw seems not to be a problem through the use of differential aileron. If adverse yaw had been present, a vertical fin would be necessary, with the possible addition of a rudder.

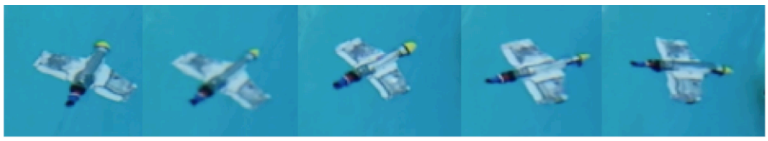

**a)** **b)** **c)** **d)** **e)**

**Figure 21. Vehicle Making a Right Turn During Testing** *Note the "slide" that occurs beginning between frames b) and c).*

## VII. Future Work

In the near future, the goal of this work will be to further understand the dynamics of the vehicle by assembling stability and control matrices. However, the primary obstacle to this is improving connectivity in the test facility. This upgrade could be accomplished in a number of ways, including tethering the vehicle or designing and constructing an underwater antenna apparatus. Once connectivity is improved, a dynamic model is just a matter of multiple flight tests. Additionally, the vehicle's buoyancy will continue to be altered in an effort to achieve more realistic flow to that of a UAV. One long-term goal is to use this vehicle for various collective control problems. A first step towards this goal would be to demonstrate controllability in a gust, as some of the new facilities at University of Maryland will permit. Additionally, construction methods will be refined to improve durability and produce multiple vehicles of similar size and shape. While there will always be improvements to be made, this work has resulted in the successful development of a underwater test platform for the low Reynolds regime, a platform that can be expanded to many projects within the research focus of the CDCL.

## Appendix I

| Table 1. Vehicle Mass Properties | |
|---|---|
| Right Wing | 885.54 g |
| Left Wing | 879.83 g |
| Left Elevon | 20.89 g |
| Right Elevon | 19.77 g |
| Pressure Vessel with Components | 1821.5 g |
| Mass in Grams | 3627.53 g |
| Mass in Slugs | 0.2486 slg |

| Table 2. Relevant Data for Calculating $I_{yy}$ | |
|---|---|
| A. Bifilar Pendulum Dimensions | |
| Distance between Wires | 9 in |
| Length of Wires | 73 in |
| | |
| B. Time Measurements | |
| Time for 10 oscillations | 23.33 s |
| Frequency | 0.4286 Hz |

| Table 3. Relevant Data for Calculating $I_{xx}$, $I_{zz}$ and $I_{xz}$ | | | | | |
|---|---|---|---|---|---|
| A. Bifilar Pendulum Dimensions | | | | | |
| Distance between Wires | 4.5 in | | | | |
| Length of Wires | 86.5 in | | | | |
| | | | | | |
| B. Time and Angle Measurements | | | | | |
| Nominal Angle (deg) | Actual Angle (deg) | Actual Angle (rad) | Oscillations | Time (s) | Frequency (Hz) |
| 90 | 90 | 1.571 | 8 | 51.88 | 0.01928 |
| 75 | 75 | 1.309 | 8 | 52.35 | 0.01910 |
| 45 | 48.9 | 0.853 | 8 | 57.33 | 0.01744 |
| 30 | 33.9 | 0.592 | 8 | 58.19 | 0.01719 |
| 15 | 13.4 | 0.234 | 8 | 60.22 | 0.01661 |
| 0 | 0 | 0.000 | 8 | 64.74 | 0.01545 |
| -15 | -16.5 | -0.288 | 8 | 65.04 | 0.01538 |
| -30 | -28.7 | -0.501 | 8 | 62.16 | 0.01609 |
| -45 | -48.7 | -0.850 | 8 | 56.48 | 0.01771 |
| -60 | -68.6 | -1.197 | 8 | 53.2 | 0.01880 |
| -90 | -89 | -1.553 | 8 | 53.76 | 0.01860 |


## Acknowledgments

Author C. J. K. would like to thank Dr. Derrick Yeo for his advising during Dr. Paley's sabbatical, as well as Levi DeVries, Frank Lagor, Raymond Bounds, his other collogues at the University of Maryland, and Albion Bowers, Robert "Red" Jensen, Victor Loera and his other mentors at NASA's Armstrong Flight Research Center.


## References


[1]Davis, W. R. Jr., Kosicki, B. B., Boroson, D. M., and Kostishack D. F. "Micro Air Vehicles for Optical Surveillance," *The Lincoln Laboratory Journal*, Vol. 9, No. 2, 1996, pp. 197-214.

[2]Anderson, J. D., *Fundamentals of Aerodynamics*, 5th ed., New York, 2007, Chap. 1.

[3]Mattey, R. A., "Bifilar Pendulum Technique for Determining Mass Properties of Discos Packages," Naval Plant Representative Office, Rept. TG 1252, John Hopkins University, Applied Physics Laboratory, MD, July 1974.

[4]Bounds, R., "Space Perch: A Human-Robot Interaction Testbed for Communication-Constrained Environments," AIAA Region I Conference 2014, (submitted for Publication)

[5]Jiang, S., and Georgakopoulos S., "Electromagnetic Wave Propagation into Fresh Water," *Journal of Electromagnetic Analysis and Application*, No. 3, 2011, pp. 261-266.